STUDY ON CORROSION RESISTANCE OF CARBON NANOTUBES REINFORCED Al_2O_3 COATING

Nguyen Van Tuan[1, *], Ly Quoc Cuong[1], Le Thu Quy[2], Pham Thi Ha[1], Pham Thi Ly[1]

[1]*Institute for Tropical Technology, VAST, 18, Hoang Quoc Viet, Cau Giay, Ha Noi, Viet Nam*

[2]*National Key Laboratory for Welding and Surface Treatment Technologies, NARIME, 4 Pham Van Dong, Cau Giay, Ha Noi, Viet Nam*

[*]Email: *nvtuan@itt.vast.vn*

Received: 11 August 2017; Accepted for publication: 7 October 2017

ABSTRACT

This paper presents our research on the reinforcement with 1 % of carbon nanotubes (CNT) for a ceramic Al_2O_3 coating applied by air plasma spray (APS) on CT3 steel. The corrosion resistances of both CNTs reinforced and non-CNTs reinforced Al_2O_3 coatings were investigated by using different such techniques as: potentiodynamic polarization; electrochemical impedance spectroscopy (EIS); salt spray and erosion corrosion tests.

The obtained results show positive effects of CNT to improve the corrosion protection of the Al_2O_3 coating: time of appearance of first rust points on the surface in the salt spray test increased from 2 hours for pure Al_2O_3 coating to 24 hours for the CNTs-Al_2O_3 one; the erosion-corrosion resistance of the CNTs-Al_2O_3 coating increased about 17 % in comparison with the one of the Al_2O_3 coating.

Keywords: Al_2O_3 coating; air plasma spray; carbon nanotubes

1. INTRODUCTION

Plasma spray is one of the thermal spray methods that are commonly used to create coatings with advanced surface properties. The technique can create a variety of coatings such as metal coatings, ceramic coatings and metallic ceramic coatings [1]. Plasma coatings are mainly used in erosive, corrosive and high temperature environments [2 - 5].

Al_2O_3 coating was prepared by the plasma spray technique with heterogeneous structure. Inside the coating, there are always defects, cracks and micropores which affect the working capability of the coating [6 - 8]. The properties of the coating, especially the corrosion resistance, can be enhanced by treating the coating's defects and micropores.

The use of reinforcing materials to enhance the properties of thermal coatings, including plasma coating has been focused on in recent years. One of ideal reinforcing materials for plasma coating is carbon nanotubes (CNTs) due to its excellent mechanical and thermal

properties. CNTs have special properties depending on the structures, such as being 6 times lighter but 100 times more durable than steel; elastic modulus of up to 1 TPa which is equivalent to that of diamond; high temperature resistance (about 2800°C in vacuum and 700 °C in air); high thermal conductivity (about 3000 W/m.K) [9]. The activity of incorporating this material into Al_2O_3 plasma coating to enhance the properties of the coating has been studied by many scientists [10 - 14].

Recently, Rakesh Goyal *et al.* used CNTs to reinforce plasma Al_2O_3 coating (CNTs/Al_2O_3). The coating was studied for application in boiler industry. The obtained results showed that, the porosity of the coating with 1.5 % CNTs reinforcement and without CNTs reinforcement was 3.99 % and 4.18 % respectively [15].

In Vietnam, the microstructure and mechanical properties of the CNTs/Al_2O_3 plasma coating have been studied recently by Pham Thi Ha *et al.* [16]. However, its corrosion properties have not been investigated. Therefore, in this paper, we will focus on surveying the corrosion properties of CNTs/Al_2O_3 coating. In addition, the corrosion resistance of non-CNTs reinforced Al_2O_3 will also be studied simultaneously for comparison purpose.

2. EXPERIMENTAL

2.1. Coating materials

The α-Al_2O_3 spray powder (purity of 98.5 %, dimension of 25 ÷ 75 μm) from PRAXAIR-TAFA (USA) was mixed with CNTs with a content of 1.0 %. CNTs are multi-walled in structure with purity of greater than 90 %, diameter of 20 ÷ 80 nm and length of 10 ÷ 100 μm. The material mixture was blended in a mixer for 12 hours continuously with a speed of 200 rpm. Pure Al_2O_3 powder is prepared to create coating with non-CNTs reinforced for comparison with Al_2O_3 coating with CNTs reinforcement. In addition, NiCr20 powder with grain size of 15 ÷ 45 μm (China) was sprayed as the bond coat on the CT3 steel substrates.

2.2. Preparation of coating

The NiCr20 coating (bond coating), CNTs/Al_2O_3 and Al_2O_3 coatings (top coating) were applied by 3710-PRAXAIR-TAFA air plasma spray equipment (USA) at the National Key Laboratory for Welding and Surface Treatment Technologies - NARIME. The spray parameters for creating coatings are as follows [15]:

- Current: 550 A (for both top and bond coatings),
- Potential: 50 V (for both top and bond coatings),
- Pressure of primary gas Ar: 50 psi for top coating and 45 psi for bond coating,
- Pressure of secondary gas He: 10 psi (for both top and bond coatings),
- Powder feed rate: 45 g/min for top coating and 10 g/min for bond coating.

The coatings were sprayed on the CT3 sheet plate with dimension of 50 × 50 × 3 mm after being cleaned and roughened by corundum abrasive blasting. The thickness of NiCr20 coating is about 100 μm and the one of CNTs/Al_2O_3 and Al_2O_3 coatings is about 300 μm.

2.2. Research methods

The morphology of Al_2O_3 powder before and after mixing with CNTs was studied using cathode cold field emission scanning electron microscope FESEM Hitachi S-4800 (Japan). Structures and phase compositions of Al_2O_3 and CNTs/Al_2O_3 coatings were analysis by XRD performed as follows: temperature 25 °C, the sweep angle 2θ in a ranges from 10° to 60°, measurement step angle of 0.03 ^{o}/s, using Cu radiation. The cross-sectional structure of the coatings was analyzed using optical microscope Axiovert 40 Mat (Germany). The corrosion resistance of the coatings was studied by salt spray test in accordance with ASTM B117 standard and electrochemical techniques including electrochemical impedance spectroscopy (EIS) and electrochemical polarization measurements in NaCl 3.5 % solution. The EIS spectra were conducted in a frequency range of 10^6 to 10^{-2} Hz. The polarization curve was measured in a range of 0.2 - 0.4 V vs E_{ocp} with a scanning speed of 0.2 mV/s on electrochemical measuring equipment Biologic VSP 300 (France). The erosion corrosion resistance of the coatings was tested in a slurry flow of H_2SO_4 pH2 solution containing 3 % SiC solid grains with a rotational speed of 1040 m/min (4 m/s) for 168 hours [17, 18]. The mass loss during erosion corrosion test was monitored over time with analytical balance of 0.0001 g accuracy.

3. RESULTS AND DISCUSSION

3.1. Structural morphology of Al_2O_3 and CNTs/Al_2O_3 powders

The structural morphology of Al_2O_3 and CNTs/Al_2O_3 powders is shown in Figures 1 and 2.

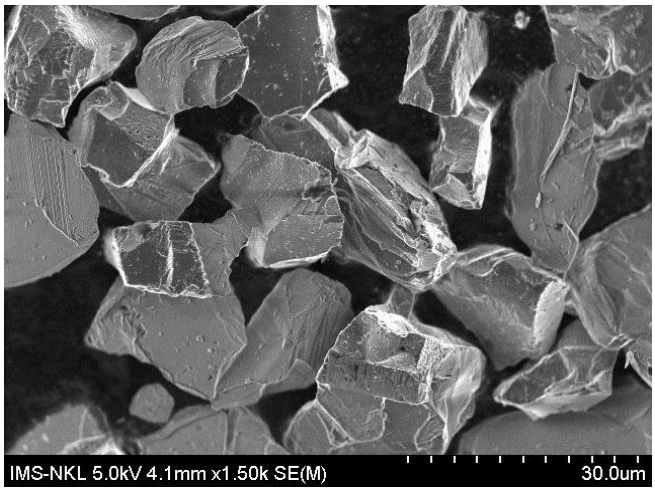

Figure 1. SEM image of Al_2O_3 powder before mixing with CNTs.

The SEM images showed that, Al_2O_3 grains, before and after mixing with CNTs, are polygonal in shape with an average size of about 30 μm. On the other hand, CNTs, after mixing with Al_2O_3 powder, have distributed quite evenly on the surfaces of Al_2O_3 grains. The enlarged image of CNTs/Al_2O_3 powder sample (Figure 2, on the right) show that CNTs in the mixture remain in tube form without breaking the characteristic structure during the process of mixing with Al_2O_3 powder.

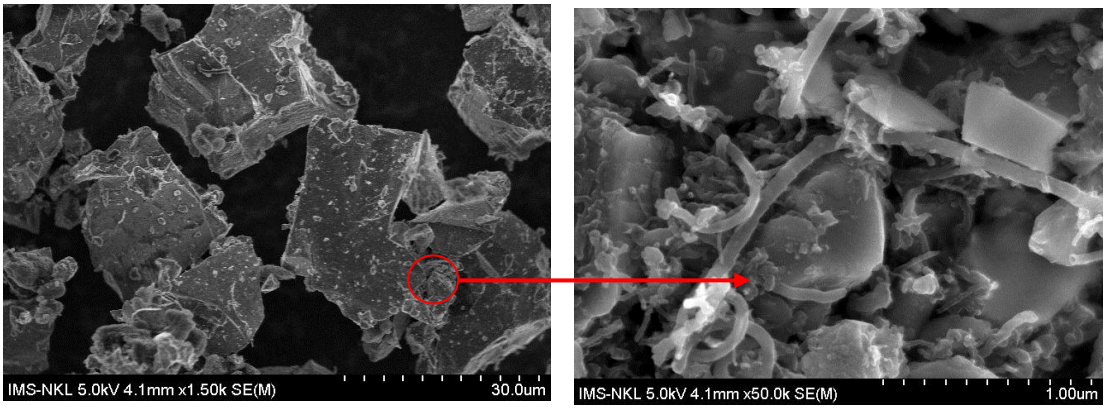

Figure 2. SEM image of Al_2O_3 powder after mixing with 1 % CNTs.

3.2. Structure and phase composition of CNTs/Al_2O_3 coating

The results of analyzing structures and phase compositions of Al_2O_3 and CNTs/Al_2O_3 coatings are shown in Figure 3.

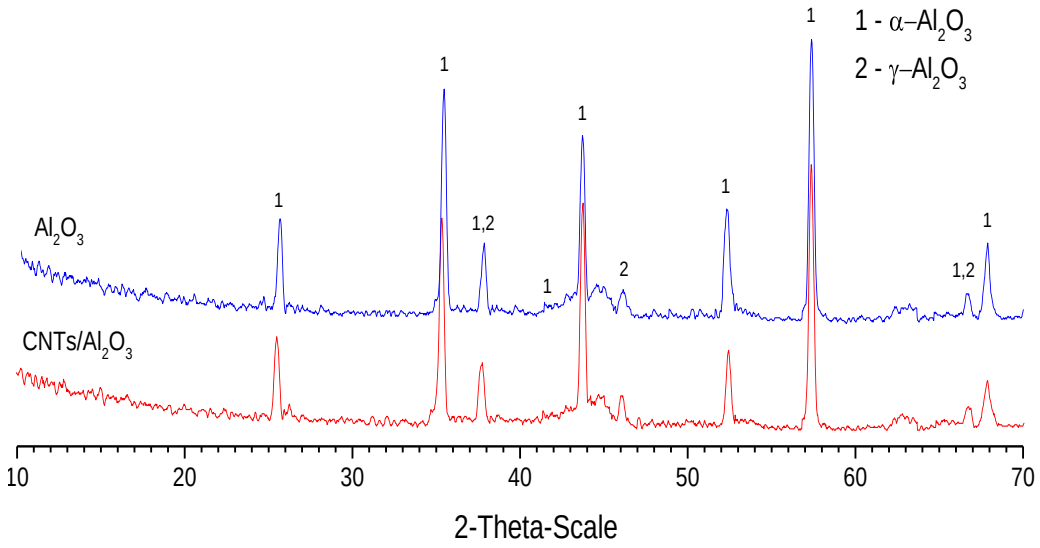

Figure 3. XRD of Al_2O_3 powder after mixing with CNTs.

The XRD results showed that, in coatings, besides the α-Al_2O_3 main phase composition, there was a presence of γ-Al_2O_3 phase composition due to the effect of high temperature in the plasma spray process, one part of α-Al_2O_3 phase changed to γ-Al_2O_3 phase. The peaks at the angles 2θ of 37.5; 46.2 and 67.6 are typical peaks of γ-Al_2O_3 phase. However, the characteristic peaks of CNTs do not appear in XRD spectrum because CNTs dispersed among Al_2O_3 grains that make detecting CNTs by XRD method more difficult (its content is below the detection limit of the XRD equipment).

3.3. Salt spray resistance

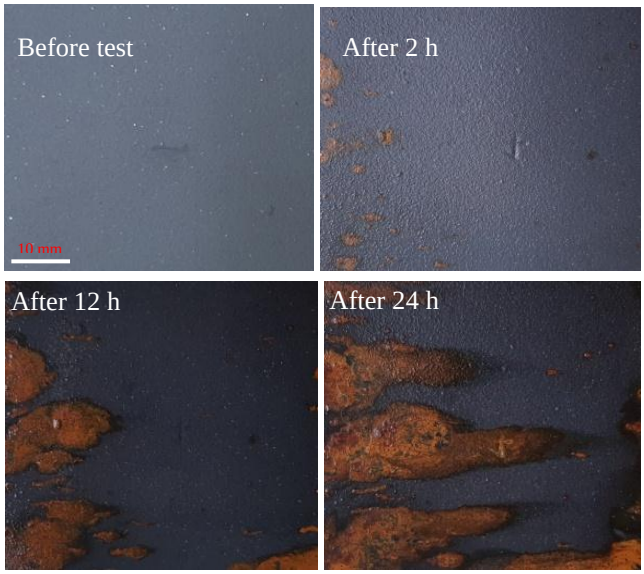

Figure 4. Surface change of Al_2O_3 coating during the salt spray test.

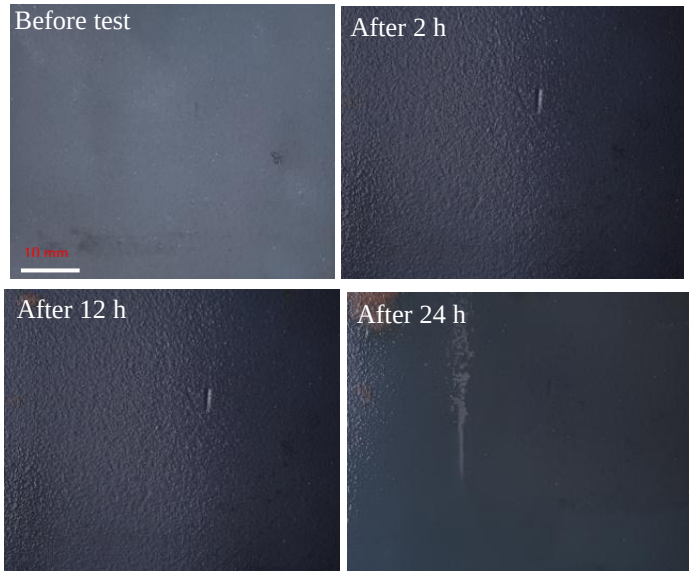

Figure 5. Surface change of CNTs/Al_2O_3 coating during the salt spray test.

After conducting salt spray test for 24 hours with 5 % NaCl solution, the results of surface observation of the CNTs/Al_2O_3 and Al_2O_3 coatings are shown in Figures 4 and 5.

One can see that there is a significant difference in corrosion protection of CNTs reinforced and non-CNTs reinforced coatings in salt spray test. For non-CNTs reinforced coating, red rust spots appeared on its surface after 2 hours of test. For CNTs reinforced coating, red rust spots appeared on its surface after 12 hours of test, which indicates that CNTs in the coating have

improved the corrosion protection of the coating. According to the research results of Xinhua L. *et al*. [10], CNTs in Al_2O_3 coating have formed bridges that help to reduce defects and porosity of the coating, thus improve its corrosion protection. To further clarify this result, we have captured the cross-sectional structure of the coating on the optical microscope Axiovert 40 Mat (Figure 6).

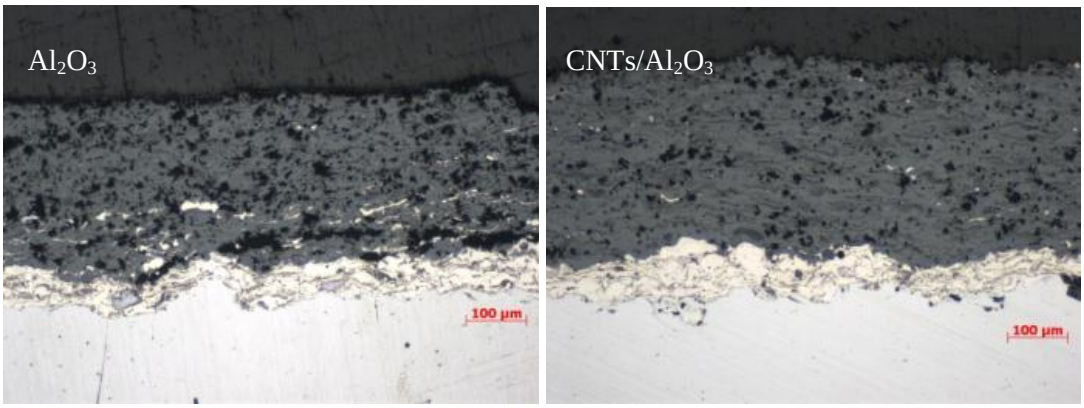

Figure 6. Cross-sectional structures of Al_2O_3 and CNTs/Al_2O_3 coatings.

The observation of cross-sectional structures of the coatings by optical microscope reveal that the pure Al_2O_3 coating contain more micropores than the coating with CNTs reinforcement. The large number of micropores inside the Al_2O_3 coating has facilitated a rapid penetration of NaCl solution through the coating causing corrosion for the steel substrate. Therefore, it can be seen that, the corrosion products of the steel substrate appeared on the surface of Al_2O_3 coating after just 2 hours of test.

The results of polarization and EIS measurements for coatings in 3.5 % NaCl solution presented below will clarify the results obtained above.

3.4. Electrochemical measurement

The coated samples with the surface 1 cm^2 were immersed in 3.5 % NaCl solution for about 30 minutes prior to EIS and polarization measurements.

Figure 7 presents the Nyquist plots of EIS spectra of Al_2O_3 and CNTs/Al_2O_3 samples. This figure also gives the most suitable equivalent circuit used to fit EIS data. The continuous curves represent the plots after fitting using EC-LabV11.02 software. In the equivalent circuit, R_s defines the equivalent resistance of the electrolytic solution; R_1Q_1 defines the resistance and capacitance of coating; R_2Q_2 defines the resistance and capacitance of boundary between coating and steel substrate [19].

Table 1. Fit data from the EIS measurement through corresponding equivalent circuit.

Sample	R_s, Ω	Q_1x10^{-3}	a_1	R_1, Ω	Q_2x10^{-3}	a_2	R_2, Ω
M1	6.886	16.51	0.8179	1334	3.228	0.3278	338.1
M2	114.8	5.24	0.7575	2437	2.82	0.625	2742

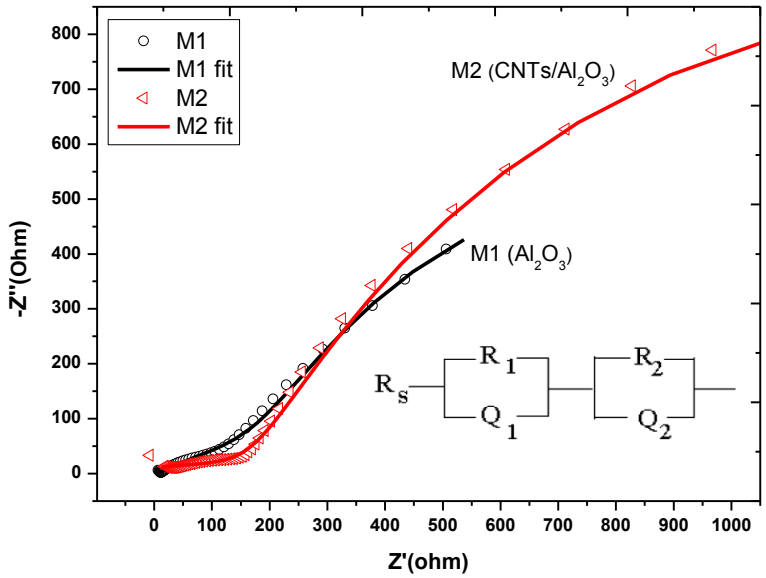

Figure 7. Nyquist diagram of Al_2O_3 and CNTs/Al_2O_3 coating measured in 3.5 % NaCl solution.

Table 1 shows the calculated values of coatings, the results show that, the resistance in the micropores (R_1) as well as the typical resistance of eroded steel substrate of CNTs reinforced coatings are 2-8 times higher than those of non-CNTs reinforced coatings.

The polarization curves of Al_2O_3 and CNTs/Al_2O_3 samples measured in 3.5 % NaCl solution are shown in Figure 8.

Table 2 summarizes the corrosion parameters obtained from the electrochemical polarization curves by EC-LabV11.02 software. The research results show that, Al_2O_3 sample has more negative corrosion potential and 50 % higher corrosion current density than that of the CNTs/Al_2O_3 coating. Thus, it can be seen that, the corrosion resistance of Al_2O_3 coatings created by air plasma spray technique is significantly improved after reinforcement of CNTs. This result is quite consistent with the salt spray test results shown in section 3.3.

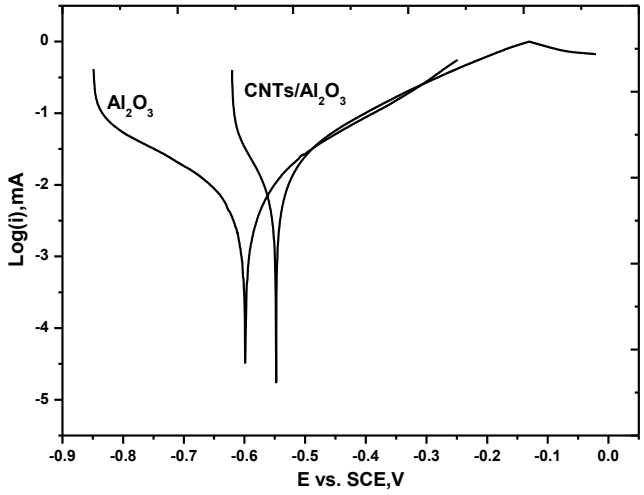

Figure 8. Polarization curves of Al_2O_3 and CNTs/Al_2O_3 coatings measured in 3.5 % NaCl solution.

Table 2. Corrosion parameters from polarization curve measurement.

Sample	E_{corr}, mV/SCE	I_{corr}, μA/cm^2
Al_2O_3	-600	6.6
CNTs/Al_2O_3	- 548	4.3

3.5. Erosion corrosion resistance

Figure 9 shows the results of the erosion corrosion resistance test for the coating over time. The result shows that, the mass loss of Al_2O_3 sample is higher than that of CNTs/Al_2O_3 one at all measuring times after 24 - 168 hours of test. This indicates that the erosion corrosion resistance of CTNs reinforced coating is higher than that of non-CTNs reinforced coating.

After 168 hours of test, the mass loss of CNTs/Al_2O_3 coating is 270 mg while the mass loss of Al_2O_3 coating is 328 mg. Therefore, the erosion corrosion resistance of CTNs reinforced Al_2O_3 coating is about 17 % higher in comparison with that one of non- CNTs reinforced coating. The CNTs forming bridges between grains in the coatings makes not only a reduction of the porosity of the coating but also an increase in bonding between grains in the coatings, thereby it would increase the erosion corrosion resistance of the coating. This shows that CNTs help to improve the corrosion protection and erosion corrosion resistance of the coating. Thus, CNTs/Al_2O_3 coating may be used as a protective coating for machine parts operated in corrosive environments with erosion factor.

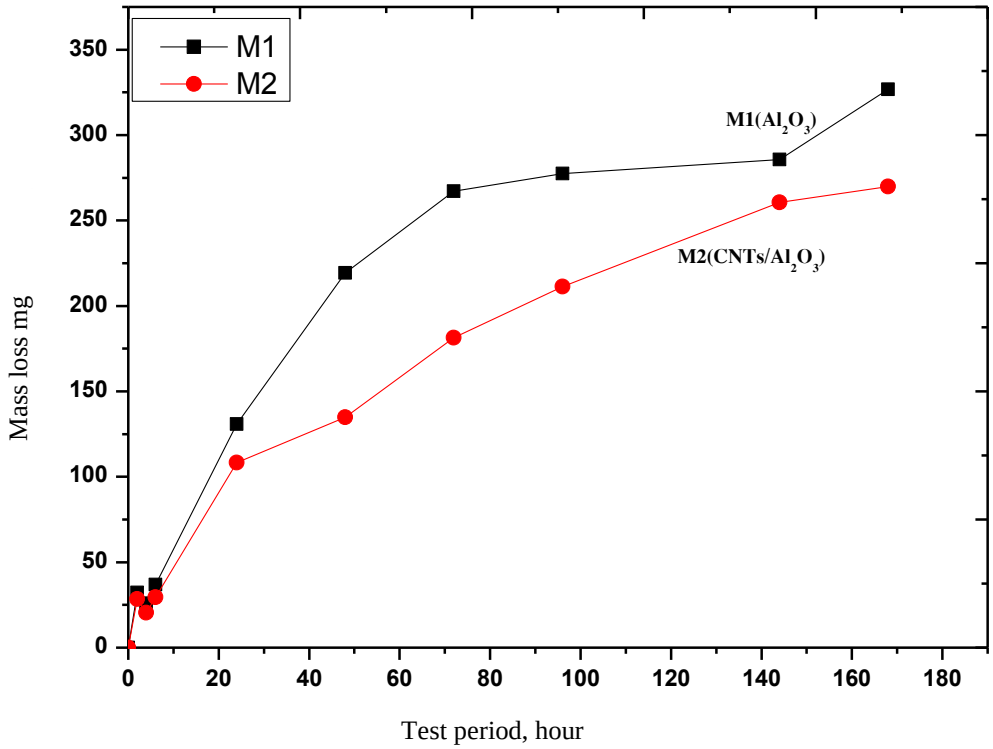

Figure 9. Erosion corrosion resistance of coatings.

4. CONCLUSIONS

After mixing with Al_2O_3 powder, CTNs are quite evenly distributed in the powder mixture and the CTNs' characteristic structures are not broken.

The corrosion protection of CNTs/Al_2O_3 coating is higher than that of Al_2O_3 coating.

The erosion corrosion resistance of CNTs/Al_2O_3 coating is about 17 % higher than that of Al_2O_3 coating.

Acknowledgements. The costs of this work were supported by the Institute for Tropical Technology, Vietnam Academy of Science and Technology.

REFERENCES

1. Sidhu B.S., Puri D., Prakash S. - Mechanical and metallurgical properties of plasma sprayed and laser remelted Ni–20Cr and Stellite-6 coatings, J. Mater. Process Technol. **159** (2005) 347–355.
2. Leon L. Shaw, Daniel Goberman, Ruiming Ren, Maurice Gell, Stephen Jiang, You Wang, Xiao T. D., Strutt P. R. - The dependency of microstructure and properties of nanostructured coatings on plasma spray conditions, Surface and Coatings Technology **130** (2000) 1-8.
3. Westergard R., Erickson L. C., Axe N., Hawthorne H. M., Hogmark - The erosion and abrasion characteristics of alumina coatings plasma-sprayed under different spraying conditions, Tribol Int. **31** (1998) 271-279.
4. Celik E., Sengil I.A., Avci E. - Effects of some parameters on corrosion behaviour of plasma sprayed coatings, Surface and Coatings Technology **97** (1997) 355-360.
5. Gao Y., Xu X., Yan Z., Xin G. - High hardness alumina coatings prepared by low power plasma spraying, Surface and Coatings Technology **154** (2002) 189-193.
6. Yin Z. J., Tao S.Y., Zhou X. M., Ding C. X. - Evaluating microhardness of plasma sprayed Al_2O_3 coating using Vickers indentation technique. J Phys D Appl Phys. **40** (2007) 7090-7096.
7. Zhao L.D., Seemann K., Fischer A., Lugscheider E. - Study on atmospheric plasma spraying of Al_2O_3 using on-line particle monitoring, Surface and Coatings Technology. **168** (2003) 186-190.
8. Guessasma S, Montavon G, Coddet C. - Velocity and temperature distributions of alumina–titania in-flight particles in the atmospheric plasma spray process, Surface and Coatings Technology **192** (2005) 70-76.
9. Balani K., Agarwal A. - Process map for plasma sprayed aluminum oxide - carbon nanotube nanocomposite coatings, Surface and Coatings Technology **202** (2008) 4270-4277.
10. Xinhua L, Yi Z, Chuanxian D, Pingyu Z. - Effects of temperature on tribological properties of nanostructured and conventional Al_2O_3-3 wt.% TiO_2 coatings, Wear. **256** (2004) 1018-1025.
11. Anup Kumar Keshri, Arvind Agarwal. - Wear behavior of plasma-sprayed carbon nanotube-reinforced aluminum oxide coating in marine and high-temperature environments, Journal of Thermal Spray Technology **20** (2011) 1217-1230.

12. Asadi.S. - Spread data analysis of Aluminum oxide splats reinforced with carbon nanotubes, Iranian Journal of Materials Science and Engineering **11** (2014) 72-79.
13. Anup Kumar K, Arvind A. - Splat morphology of plasma sprayed aluminum oxide reinforced with carbon nanotubes: A comparison between experiments and simulation, Surface and Coatings Technology **206** (2011) 338-347.
14. Bai Y, Yang JF, Lee SW, Chen H, Yu FL, Zhang J. - Spray-drying of alumina powder for APS: effect of slurry properties and drying conditions upon particle size and morphology of feedstock, Bulletin of Materials Science **34** (2011) 1653-1661.
15. Rakesh G, Buta S S, Vikas C. - Characterization of plasma-sprayed carbon nanotube (CNT) reinforced alumina coatings on ASME-SA213-T11 boiler tube steel, Int. J. Adv. Manuf. Technology, DOI 10.1007 (2017).
16. Pham Thi Ha, Nguyen Van Tuan, Phạm Thi Ly, Le Thu Quy, Research on the production of nanocomposite aluminum oxide carbon nanotubes coating ($CNTs/Al_2O_3$) by plasma spray technology, Vietnam Journal of Chemistry **54** (5) (2016) 570-574.
17. Abbade N. P., Crnkovic S. J. - Sand- water slurry erosion of API. 5L X65 pipe steel as quenched from intercrid temperature, Tribology International. **33** (2000) 811-816.
18. Fang Q., Xu H., Sidky P. S., Hocking M. G. - Erosion of ceramic materials by sand/water slurry jet, Wear **224** (1999)183-193.
19. Suegama P.H, Fugivara C.S, Benedetti A.V, Ferna'dez .J, Delgado. J, Guilemany J.M. - The influence of gun transverse speed on electrochemical behaviour of thermally sprayed Cr_3C_2–NiCr coatings in 0.5M H_2SO_4 solution, Electrochimica Acta **49** (2004) 627–6341.